Agricultural and Forest Meteorology 263 (2018) 267–275

Contents lists available at ScienceDirect

Agricultural and Forest Meteorology

journal homepage: www.elsevier.com/locate/agrformet

Short communication

On the calculation of daytime CO_2 fluxes measured by automated closed transparent chambers

Peng Zhao[a,*], Albin Hammerle[a], Matthias Zeeman[b], Georg Wohlfahrt[a]

[a] Institute of Ecology, University of Innsbruck, Austria
[b] Karlsruhe Institute of Technology (KIT) Atmospheric Environmental Research Institute of Meteorology and Climate Research (IMK-IFU), Germany

ARTICLE INFO

Keywords:
Net ecosystem exchange
Carbon dioxide
Chamber measurement

ABSTRACT

Automated transparent chambers have gained increasing popularity in recent years to continuously measure net CO_2 fluxes between low-statured canopies and the atmosphere. In this study, we carried out four field campaigns with chamber measurements in a variety of mountainous grasslands. A mathematic stationary point (or critical point, a point at which the derivative of a function is zero) in the CO_2 mixing ratio time series was found in a substantial fraction of the measurements at all the sites, which had a significant influence on the performances of the regression algorithms. The stationary point was probably due to condensed water on the inner wall of the chamber dome, which reduced the solar radiation and resulted in a reversal of the CO_2 mixing ratio time series in the chamber (so called *Clouded-Glass Effect* or CGE in this study). This effect may be the cause of the observed underestimation of daytime CO_2 fluxes when using common linear and exponential regression models on continuous automated chamber observations. In order to avoid biased flux estimation of daytime CO_2 fluxes, we introduced a linearly increasing term to the exponential function so as to compensate for the influence of the CGE, which gives acceptable model errors and improves the CO_2 flux estimation by 5% for temperate mountainous grasslands. We conclude that exponential regression models should be favoured over linear models and recommend to account for the effects of CGE by either excluding ambiguous observations from the flux computations where stationary points can be identified in the CO_2 mixing ratio time series, or by adding a linearly increasing term to the exponential regression model.

1. Introduction

Quantification of ecosystem carbon dioxide (CO_2) fluxes plays a key role in the estimation of green-house gases' contribution to global warming. The closed chamber technique, carried out with a bottomless sealed container sitting on the soil surface or low-statured canopies, represents a common approach to estimate CO_2 flux (Denmead, 2008). Manually operated chambers have been widely used owing to their low cost, but are very time-consuming to operate. In recent years automated chambers have been applied (Rochette and Hutchinson, 2005) and various systems have been developed over the years (Koskinen et al., 2014; Savage et al., 2014; Görres et al., 2016). Automated chambers can continuously measure CO_2 fluxes with a relatively high frequency (e.g. 30-60 min) over the long term. Furthermore, the development of automated transparent chamber allows continuous measurement of the net ecosystem CO_2 change (NEE), which is necessary for seasonal and annual carbon budget estimation (Riederer et al., 2014).

In an ecosystem, CO_2 is released to the atmosphere by respiration from plants, microorganisms surrounding the plant roots, and heterotrophic decomposition of soil organic matter and plant litter, while during daytime CO_2 is removed from the air by the vegetation photosynthesis. The net CO_2 exchange, i.e. the sum of plant photosynthesis and the ecosystem respiration, can be estimated with the information from the initial slope of the time series of CO_2 mixing ratio in the chamber measurement. Negative flux values mean net CO_2 uptake and positive flux values mean net CO_2 release. Owing to the improvement of the measurement techniques, many chamber design effects have been eliminated in recent years that could systematically invalidate trace gas flux observations, such as inconsistencies resulting from pressure gradients between inside and outside the chamber at various wind speeds (Rochette and Hutchinson, 2005; Xu et al., 2006; Pihlatie et al., 2013). However, some challenges and different opinions still exist. For instance, Riederer et al. (2014) demonstrated that chamber measurements were biased in comparison with eddy-covariance measurement during night time, and Brændholt et al. (2017) found that soil CO_2 effluxes were overestimated by closed chamber measurements at low

* Corresponding author.
E-mail address: pzhao@pzhao.net (P. Zhao).

https://doi.org/10.1016/j.agrformet.2018.08.022
Received 2 January 2018; Received in revised form 21 August 2018; Accepted 23 August 2018
Available online 08 September 2018

atmospheric turbulence, but Görres et al. (2016) indicated that modern automated chambers are capable to provide reliable night time CO_2 fluxes, and Galvagno et al. (2017) reported that chamber measurements agreed with the eddy-covariance method after quality control and proper corrections. With closed chambers, the CO_2 flux is estimated as the rate of change in CO_2 mixing ratio inside the chamber. A linear regression of the gas concentration against time is often applied to derive the flux owing to the simplicity (Hendriks et al., 2007, 2010), but Kutzbach et al. (2007) considered the exponential regression in CO_2 concentration data of chamber measurements as the most accurate approach which is practicable in complex vegetation-soil systems against linear regression even if the closure time is short. Later Koskinen et al. (2014) argued that the linear fit is simple and robust and no worse than polynomial fitting in their study. Recently Moffat and Brümmer (2017) reported the underestimation by the linear fit and proposed an improved parameterization of the exponential equation with physically meaningful parameters.

Most of these studies in the literature were focused on the trace gas fluxes measured with dark chambers at bare soil surfaces rather than transparent chambers on vegetated surfaces for which a standardized procedure for data processing and quality control is still unavailable (Vargas et al., 2011; Galvagno et al., 2017). The rate of change in the CO_2 mixing ratio in a closed chamber depends on the soil and plant respiration, gross photosynthesis of the plants, and the leakage directly at the chamber components or via the soil pore space (Kutzbach et al., 2007). Modelling of the CO_2 concentration changes over time in the chamber headspaces is more complicated for vegetated surfaces than for bare soil surfaces since additional processes such as photosynthesis and plant respiration have to be considered (Kutzbach et al., 2007). The CO_2 flux from the soil to the headspace air is mainly driven by molecular diffusion, which depends on the soil CO_2 diffusivity, the CO_2 concentration difference between the CO_2-enriched soil pore space and the headspace air, the air temperature and pressure (Matthias et al., 1978; Kutzbach et al., 2007). Photosynthesis is dependent on irradiation, which limits the electron transport rate at the chloroplast, and on the intercellular CO_2 concentration, which limits the activity of Rubisco (Farquhar et al., 1980). For both the non-irradiation-limited photosynthesis situation and the irradiation-limited photosynthesis situation, the evolution of CO_2 mixing ratio over time was proposed to be simply described against time by an exponential function (Kutzbach et al., 2007). However, the curvature of the nonlinear curves of CO_2 mixing ratio evolution for a substantial percentage of the experiments cannot be explained with the proposed theoretical model (Kutzbach et al., 2007). Irradiation, temperature, and humidity in a transparent chamber might be affected during daytime, which could bring unexpected uncertainties in regression and subsequently in flux estimation.

In this paper, CO_2 flux measurements with automated transparent chambers were carried out at a variety of grasslands. We intended (1) to test the performance of automated transparent chambers, (2) to find the optimal calculation procedure from linear and exponential regressions for daytime CO_2 flux estimation, and (3) to improve the reliability of daytime chamber CO_2 flux estimation over short-statured canopies.

2. Methods

2.1. Sites

Field campaigns were carried out at four grassland sites across the Alps in Italy, Austria and Germany episodically in 2015 and 2016 (Table 1). These sites covered a range of terrain types which were typical for mountains with varying degrees of complexity.

The experiment at Monte Bondone site (FLUXNET site code: IT-MBo, abbreviated as MB in this study) was performed in October, 2015. MB is situated on a typical low productive meadow on a mountain plateau in north Italy (Marcolla et al., 2011). The mean annual temperature is 5.5 °C and the total mean annual precipitation is 1189 mm.

Table 1
Site information.

Site	Coordinates	Elevation	Measurement periods
Monte Bondone (MB)	46° 01′N, 11° 04′E	1550 m	Oct. 2015
Hochhäuser (HH)	47° 17′N, 11° 38′E	1010 m	May 2016
Fendt (FT)	47° 50′N, 11° 04′E	595 m	July 2016
Neustift (NS)	47° 07′N, 11° 19′E	970 m	Oct. 2016

The vegetation is dominated by *Festuca rubra (L.), Trifolium sp. (L.), and Nardus stricta (L.)*. The canopy height was 0.19 m during the campaign.

The field campaign at Hochhäuser site (HH) was carried out in May 2016. HH is situated on a steep (27°) slope of the mountainous area in the Inn Valley in Austria (Rotach et al., 2017). Daily mean temperature typically ranges from −1 °C in winter to +20 °C in summer. The total mean annual precipitation is about 1100 mm. The canopy height was 0.35 m during the campaign.

The field measurement took place at Fendt site (FLUXNET site code: DE-Fen, abbreviated as FT in this study) during the ScaleX campaign in July 2016 (Wolf et al., 2017). FT is located in a drained alluvial area with increasing mountainous features in Germany and is part of the TERrestrial Environmental Observatory (TERENO) network (Zacharias et al., 2011; Zeeman et al., 2017). The canopy height was 0.20 m during the campaign.

The experiment at Neustift (FLUXNET site code:AT-Neu, abbreviated as NS in this study) was performed in October 2016. NS is located in the middle of the flat bottom of the Stubai Valley in Austria with an annual temperature of 6.5 °C and precipitation of 852 mm (Wohlfahrt et al., 2008). The soil is a Fluvisol (FAO classification) covered mainly with graminoid (*Dactylis glomerata, Festuca pretensis, Phleum pratensis, Trisetum flavescens*) and forb (*Ranunculus acris, Taraxacum officinale, Trifolium repens, Trifolium pratense, Carum carvi*) species. The canopy height was 0.10 m during the campaign.

2.2. Instrumentation

This study used three automated closed transparent chambers (LI-8100-104C, LI-COR Biosciences, Lincoln, NE USA) to measure net CO_2 fluxes between the surface and the atmosphere. The chamber had a surface area of 317.8 cm^2, a transparent dome with a height of 33 cm, and a headspace volume of approximately 4080 cm^3, which varied a little due to different offsets of the cylindrical collars installed in the soil. The chamber was designed to avoid perturbations to the disturbance from the surrounding environmental conditions such as the heating for the surface under the base plate, and the pressure pulse at chamber closing (Riederer et al., 2014; Görres et al., 2016).

At MB, HH, and NS the chambers were operated under the control of a data-logger (CR1000, Campbell Scientific, Inc., Logan, UT, USA)-microcontroller (Arduino MEGA2560, Smart Projects, Ivrea, Italy) system. Air was circulated from the chamber to an infra-red gas analyzer (IRGA, Li-840a, LI-COR, Lincoln, NE, USA) and then returned to the chamber with a flow rate of 1 l min^{-1}. When a measurement started, the sampling system was flushed with ambient air for 1 min as a pre-purge process, including a closing process time of 15 s. Afterwards the chamber dome was moved by a mechanical arm and then rested on the collar installed one day before the experiment started. Then a 150-s measurement began with the first 15 s as the deadband, and the subsequent time as the observation length. After one measurement ended, the chamber dome was lifted by the arm and rotated 180° away from the collar as an open status, and the control system switched the air-sampling line to another chamber by solenoid valves. This protocol was repeated every 30 min. The CO_2 mixing ratio was recorded every 3 s, and was converted into dry mole fraction on the data-logger. At FT site, the chambers were managed by a control unit (LI-8100A, LI-COR, Lincoln, NE, USA) and a multiplexer (LI-8150, LI-COR, Lincoln, NE,

USA). The CO_2 mixing ratio was recorded at 1 Hz. The raw datasets were quality controlled with the software package by Lüers et al. (2014).

As ancillary information, the latent heat fluxes were measured with the eddy-covariance technique at each site. The instrumentation and flux calculation were well documented in Marcolla et al. (2011) for MB, Wohlfahrt et al. (2008) for NS, and Mauder et al. (2013) and Zeeman et al. (2017) for FT. At HH, the eddy-covariance system was equipped with a three-dimensional sonic anemometer (CSAT3, Campbell Scientific, Inc., Logan, UT, USA) and an open-path infra-red gas analyzer (Li-7500, Li-Cor, Lincoln, NE, USA) at 1.9 m above the ground, which performed the measurement at 20 Hz. Half-hourly mean latent heat fluxes were calculated as the covariance between the turbulent departures from the mean of the vertical wind speed and the H_2O mixing ratio using the post-processing software EdiRe (University of Edinburgh). The post-processing procedure and quality control followed Hammerle et al. (2007), who successfully carried out eddy covariance measurement at a grassland site with a steep slope in the same region and concluded that measurements made above a mountain meadow on a steep slope are of similar quality as fluxes measured over flat terrain after appropriate quality control.

2.3. Flux calculation

The CO_2 flux (F, μmol $m^{-1}s^{-1}$) was calculated as (LI-COR, 2010)

$$F = \frac{10VP_0\left(1 - \frac{W_0}{1000}\right)f_0}{RS(T_0 + 273.15)}, \quad (1)$$

where f_0 is the initial rate of change in water-corrected CO_2 mole fraction (C, μmol mol^{-1}) inside the chamber, i.e. $f_0 = \partial C/\partial t|_{t=t_0}$, V (cm^3) is the chamber volume, S (cm^2) is soil surface area, T_0 (°C) is the initial air temperature, P_0 (kPa) is the initial air pressure, W_0 (mmol mol^{-1}) is the initial water vapor mole fraction, and R (= 8.314 Pa m^3 K^{-1} mol^{-1}) is the ideal gas constant. The subscript 0 means a variable's value at $t = t_0$, where t_0 is the initial time.

The linear regression is a common algorithm to estimate f_0 owing to its simplicity. The least squares method is applied to fit a straight line presented as

$$C = a_0 + a_1 t, \quad (2)$$

where a_0 and a_1 are the intercept and slope of the line, respectively, and t is the measurement time. Thus f_0 can be calculated as

$$f_0 = \frac{\partial C}{\partial t}\bigg|_{t=t_0} = a_1. \quad (3)$$

The linear regression method requires a short measurement duration. In this study, we used two strategies to define the measurement time. The first strategy, which was abbreviated as Lin1, used the entire measurement, i.e. 150 s after a chamber was closed. The second method, which was abbreviated as Lin2, used the data from the beginning of a measurement to the first stationary point (i.e. the point on the graph of the function where the function's derivative is zero), which was defined by the first minimum value of a fourth-order polynomial fitted to the time series of the observed CO_2 mixing ratio.

In order to account for the disturbance by the chamber closure on the CO_2 gradient, an empirical non-linear function in an exponential form was proposed by De Mello and Hines (1994) in an exponential way and later modified as (Xu et al., 2006; LI-COR, 2010):

$$C = C_x + (C_0 - C_x)e^{-k(t-t_0)}, \quad (4)$$

where C_x is the maximum mixing ratio of CO_2 when equilibrium is established between the soil and the air in chamber, C_0 is the initial CO_2 mixing ratio computed as the intercept of a linear regression of the first 15-s CO_2 mixing ratio after the chamber closes. t_0 is the time when $C = C_0$, and k is a constant accounting for the concentration saturation rate (LI-COR, 2010). C_x, t_0 and k were fitted to the time series of the observed CO_2 mixing ratio in an iterative way using the optimization function in R language (R Core Team, 2016). Subsequently, f_0 was calculated as

$$f_0 = \frac{\partial C}{\partial t}\bigg|_{t=t_0} = k(C_x - C_0). \quad (5)$$

Similarly to the linear regression algorithms, two non-linear strategies were performed. The one using the entire measurement period was abbreviated as Exp1, and the other using the data from the beginning of a measurement to the first stationary point in the CO_2 mixing ratio time series was abbreviated as Exp2.

We used the root mean square error (RMSE) to evaluate the goodness-of-fit (GOF) for each algorithm, expressed as

$$\mathrm{RMSE} = \sqrt{\frac{1}{N}\sum_{i=1}^{N}(P_i - O_i)^2}, \quad (6)$$

where P is the predicted value, O is the observed value, and i is the ith record.

3. Results and discussion

3.1. Case studies

Two examples of CO_2 mixing ratio evolution in the chamber measurements are illustrated as case studies in Fig. 1. Both measurements took place on clear-sky days at FT site (Case A: 2016.07.11 13:12; Case B: 2016.07.15 12:12).

Case A shows an expected pattern of CO_2 mixing ratio evolution in a chamber. At the beginning of the curve in Fig. 1a, it took seconds to establish the steady air mixing after the chamber closed. Then the CO_2 mixing ratio decreased sharply due to the ecosystem net uptake of CO_2, which subsequently decreased the CO_2 gradient between the canopy and the air above, and further decreased the change rate of the CO_2 mixing ratio. Because no stationary point was found in the fourth-order fitted polynomial curve, all the four regression algorithms used the same data-set for regression. The RMSE of the linear regressions was 15.4 ppm, much greater than the exponential regressions with RMSE = 2.07 ppm. The linear regressed straight line of Lin1 and Lin2 gave a slope of -1.43 ppm s^{-1}, and the exponential curve of Exp1 and Exp2 gave an initial slope of -4.22 ppm s^{-1}. The ratio between them was 0.341:1, which indicates that the linear regressions underestimated f_0 from the exponential regressions remarkably.

Case B displayed a pattern with a remarkable reversal in C (Fig. 1e). The stationary-point time (t_s) was only 63.5 s, and the CO_2 mixing ratio increased sharply from 365 ppm at t_s to 380 ppm at the end of the measurement period. The abnormal evolution of CO_2 mixing ratio resulted in the opposite signs of f_0 between Lin1 (0.00371 ppm s^{-1}, nearly neutral) and Lin2 (-0.565 ppm s^{-1}), while Lin2 had a much smaller RMSE of (2.75 ppm) than Lin1 (6.48 ppm). RMSE of Exp1 and Exp2 were 4.7 and 1.38 ppm, respectively, both smaller than those by the linear regression methods. As Exp2 was the most reliable simulation due to the smallest RMSE in this case, we used Exp2 as reference. The ratio of the fitted slopes was Lin1: Lin2: Exp1: Exp2 = -0.00393:0.598:1.21:1.

These case studies demonstrate that (1) the exponential methods fitted the observed data better than the linear methods even if the observation length is as short as 1 min, and that (2) the rate of CO_2 mixing ratio change in a transparent chamber as well as the CO_2 flux can be underestimated by 40% in comparison with the exponential fit method, which agrees with other studies, such as N_2O flux measurements by Kroon et al. (2008), or CO_2 flux measurements by Kutzbach et al. (2007), who indicated that the initial slope of linear regressions can be as low as 40% compared to the initial slope of the exponential regression for closure times of only 2 min. According to Fick's law, the gas flux

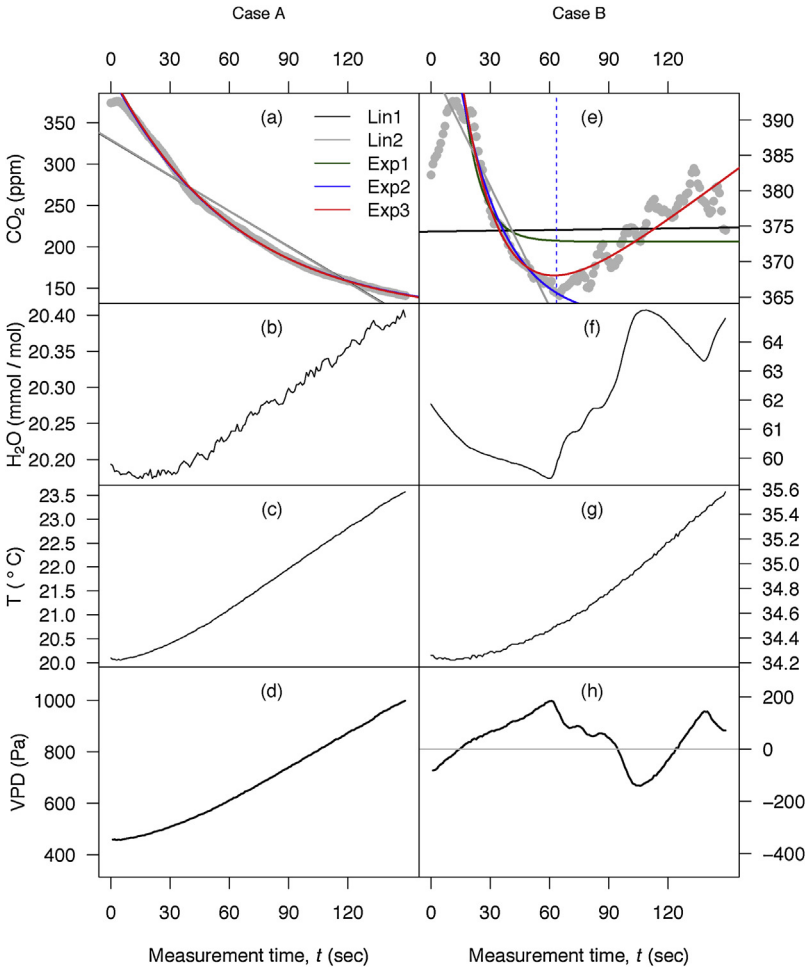

Fig. 1. Case study of the CO_2 mixing ratio evolution in chamber flux measurements. The left panel is Case A, the right panel Case B. The sub-figures a and e are two patterns of CO_2 mixing ratio evolution. Points in gray: measurements. Curves in black, gray, green, blue, and red: fitted curves by the linear and exponential regression methods abbreviated as Lin1, Lin2, Exp1, Exp2, and Exp3, respectively. These abbreviations are explained in Sections 2 and 3.2. Dotted vertical line: indicating the mathematical stationary point of the fourth-order fitted polynomial curve. The sub-figures b and f are water vapor mixing ratio, c and g are chamber air temperature, d and h are vapor pressure deficit (VPD) at the chamber wall.

is dependent on the diffusivity of the soil and the gas concentration gradient. When the chamber is closed, saturation or leakage of CO_2 could take place, resulting in a disturbance of the concentration gradient within and above the soil, which is ignored by the linear fit method. Thus, Kutzbach et al. (2007) indicated that the flux is underestimated by the linear fit method, which is inappropriate for closed-chamber methods because it seriously biases CO_2 flux estimates. Alternatively, it is suggested that the exponential function is superior because it is closer to the reality if compared to the linear regression algorithm based on a goodness-of-fit analysis (Kroon et al., 2008).

Note that although the estimated fluxes by Exp2 are not necessarily the true CO_2 fluxes, Exp2 was used as the reference, because it was the best simulation of CO_2 mixing ratio evolution. Kutzbach et al. (2007) proposed a conceptual model based on biophysical processes including the gas diffusion from the soil, the plants' photosynthesis and respiration, as well as leaks of the chamber or through the soil, and concluded that the exponential regression was the most accurate approach to reflect the CO_2 mixing ratio evolution in chamber measurements from complex vegetation-soil systems despite the possible underestimation indicated by Matthias et al. (1978) and Livingston et al. (2006).

3.2. Clouded-glass effect

The evolution of the CO_2 mixing ratio in Case B could hardly be explained by the exponential model. The CO_2 mixing ratio evolution was visually close to a roughly linear increase with noise after t_s (Fig. 1b), which was found in approximately 30% of the daytime chamber measurement in the campaigns. We mathematically added a linear term as a compensation into Eq. (4), expressed as (abbreviated as Exp3 in this study):

$$C = C_x + k'(t - t_0) + (C_0 - C_x)e^{-k(t-t_0)}, \quad (7)$$

where k' (ppm s^{-1}) is a fitting parameter.

The performance of Exp3 is displayed as the red curves in Fig. 1. In Case A, the fitted curve of Exp3 overlapped with that of Exp1 and Exp2. The exponential regressed initial slope by Exp3 was very close to Exp1 and Exp2 with $f_0 = -4.2$ ppm s^{-1} and negligible $k' = 0.0002$ ppm s^{-1}. In Case B, Exp3 captured the reversal in C, giving a fitted k' of 0.207 ppm s^{-1}, which accounted for -22% of f_0 by Exp2. RMSE of Exp3 was 2.15 ppm, smaller than that of Exp1.

To our knowledge, there is surprisingly little information in the existing literature about inexplicable curvatures of gas concentration time series in transparent chamber measurements. The most informative study mentioning such behavior of trace gas concentration in chamber measurements was by Kroon et al. (2008), who classified the gas concentration evolution into eight patterns in 25-min measurements, and discarded half of them because they were physically unexplainable. Kutzbach et al. (2007) reported that 20% to 40% of the fitted curves did not conform to the theoretical model, which was suggested to have been caused by violations of the basic assumptions of the theoretical model.

In our field campaigns, we visually observed during daytime that tiny water drops (dew) condensed increasingly on the inner wall of the chamber domes after the chamber closed until the dome of the chamber was as opaque as clouded glass, which must decrease the solar radiation received under the dome. In order to study the clouded-glass effect (CGE), the water vapor mixing ratio and the air temperature in the chamber, as well as the vapor pressure deficit (VPD) at the chamber

dome were plotted in parallel with Case A (Fig. 1b–d) and B (Fig. 1f–h). It was assumed that the dome temperature was equal to the ambient air temperature, according to which VPD was calculated. The water vapor mixing ratio (approximately 20×10^3 ppm) in the chamber rose after the chamber closed (Fig. 1b) because of the evapotranspiration of the vegetation and soil covered by the chamber dome. In the meanwhile the surface was heated, which increased the chamber air temperature, while the ambient air temperature as well as the dome temperature remained nearly constant in the 150-s measurement. In Case B the chamber air humidity was high (approximately 59–65 $\times 10^3$ ppm, Fig. 1f), therefore the difference between the chamber and ambient air temperatures resulted in the saturation of water vapor (VPD ~ 0, Fig. 1h) on the inner wall of the chamber dome. Note that negative VPD appeared in Fig. 1h, probably because the assumption that the dome temperature should equal the ambient temperature was not warranted. The dome temperature could be either higher or lower than the ambient temperature, which depends on the heating or the cooling of the air in the chamber, the specific heat capacity and the thermal conductivity of the dome. If the inner wall of the dome is heated by the warm inner air, then the true dome temperature could be higher than the ambient temperature, which results in a greater saturation water vapor pressure near the dome. Consequently, the actual VPD could be higher than the values shown in Fig. 1d and h, which could explain the negative estimated VPD values. Considering the small change rate of chamber air temperature, the deviation in the VPD estimation is slight. As a consequence, the water vapor condensed on the inner wall of the chamber dome gradually, which reduced the solar radiation in the chamber and as a consequence the photosynthesis of the vegetation (Zhao and Lüers, 2016), and thus the net exchange of CO_2 turned from negative (towards the surface) to positive (away from the surface) after t_s.

The water vapor condensation on the chamber walls was first discussed by Rochette and Hutchinson (2005), who indicated that the condensed water slightly affects the CO_2 concentration by changing the headspace volume and by absorption-desorption of CO_2, resulting in 3% overestimation of the flux. Note that Rochette and Hutchinson (2005)'s study was focused on soil respiration. For transparent chambers with plant transpiration and photosynthesis involved, the water vapor condensation could result in 22% underestimation of CO_2 flux estimation by the transparent chamber technique in the case study, if we assume that k' in Eq. (7) mainly accounts for the reversal in C by CGE.

3.3. Determination of observation length

We had in total 2435 measurements of daytime (9:00 to 15:00 LST) chamber CO_2 fluxes in the four campaigns, among which 882 measurements (i.e. 36%) showed a Case B pattern with a stationary-point time $t_s < 150$ s. The distributions of t_s values for each site are shown in Fig. 2. As none of these patterns follows a normal distribution, we use the median and interquartile range (IQR) to describe the statistics of t_s.

A stationary-point $t_s < 150$ s was found in a remarkable percentage, i.e. 33%, 29%, 40%, 40% of the measurements at FT, HH, MB, NS, respectively. The medians of t_s ranged from 64 s (NS) to 88 s (FT). Half of the number of t_s were distributed around the medians with the IQR ranging from 42 s to 59 s. The minimums of t_s ranged from 23 s (NS) to 41 s (FT). As Section 3.1 showed the influence of t_s on the flux calculation, such a substantial fraction of the measurements with small t_s indicates that the observation length for regression must be taken into consideration.

The diurnal patterns of daytime t_s for each site are shown as box plots in Fig. 3. At FT and HH sites, notable diurnal changes were found in t_s with small median values less than 80 s around mid-day (11:00 to 13:00). In other hours, t_s was relatively greater, most of which were above 90 s. At NS, although the diurnal changes in both t_s and latent heat flux were insignificant, most t_s values were smaller than 70 s in all hours of daytime.

The diunal changes in t_s were probably due to the influence of evapotranspiration. As supplementary information, the mean latent heat fluxes (the equivalent energy term of evapotranspiration) during the corresponding field campaigns from nearby eddy-covariance measurements are shown in Fig. 3 as well. At mid-day the solar radiation was strong, which enhanced the evapotranspiration and consequently resulted in the high humidity in the chamber and condensed water on the inner wall of chamber domes. Note that t_s at NS was small even when the evapotranspiration was low, probably because of the low VPD during the campaign.

The selection of observation time for chamber measurements was empirical in the literature. For instance, the observation length of CO_2 flux estimation ranged between 1.5 min to 10 min (Wohlfahrt et al., 2005; Kutzbach et al., 2007; Savage et al., 2008; Koskinen et al., 2014; Görres et al., 2016; Guidolotti et al., 2017; Kostyanovsky et al., 2018), and that of other green house gases such as CH_4 and N_2O ranged between 10 min to 25 min (Hendriks et al., 2007; Kroon et al., 2008; Savage et al., 2014). Most of the published studies on chamber CO_2 flux measurements were taken with dark chambers or at night for only ecosystem respiration. Riederer et al. (2014) deployed automated transparent chambers for CO_2 flux measurements with an observation length of 1.5 min. It was reported that the performance of fitting is strongly dependent on the selected duration of the observation (Kutzbach et al., 2007; Koskinen et al., 2014). Generally the measurement time should be as short as possible (Kutzbach et al., 2007). Our results indicated that care must be taken when using transparent chambers for daytime CO_2 flux measurement at grasslands, especially around noon time, as t_s could be smaller than one minute.

3.4. Overall performance of all algorithms

This study tested five algorithms for all four campaigns in order to investigate the difference between them (Fig. 4, using RMSE by Exp2 as reference). Most (91%) of RMSEs by both Lin1 and Lin2 regression algorithms were larger, indicating a poorer fit, than the RMSEs by Exp2. Especially, among the measurements with the stationary point $t_s < 150$ s, 93% of Lin1 RMSEs and 89% of Lin2 RMSEs were larger than Exp2 RMSEs. Regarding the exponential regressions, 84% of Exp1 RMSEs were larger than Exp2 RMSEs among those measurements with $t_s < 150$ s. Exp3 showed the best agreement with Exp2, i.e. only 30% of RMSEs were slightly larger than Exp2 RMSEs. For the measurements where no stationary point was found, Exp3 performed even better than Exp2 with lower RMSEs in some cases.

In order to investigate the influence of different algorithms on flux calculation, the fitted initial curve slopes (f_0) were used to subsequently calculate CO_2 fluxes (F). Reliable fluxes can be derived only if poorly fitted measurements are filtered before calculation. Thus, those slopes with RMSE > 5 ppm were rejected. Approximately 80% of the linear slopes and 93–98% of the exponential regressed slopes were finally accepted for calculation of the fluxes in the four campaigns.

The averaged daytime CO_2 flux (F) patterns derived from the five algorithms are shown in Fig. 5. Obviously the fluxes fall into two groups as a linear regression group and an exponential regression group. Although F values derived from Lin2 are slightly closer (than Lin1) to those from exponential regressions, both Lin1 and Lin2 significantly underestimated F from the exponential models throughout the daytime, especially at noon. The mean ratio of F_{Lin1} / F_{Exp2} is 0.32, ranging between 0.13 and 0.42, while the mean ratio of F_{Lin2} / F_{Exp2} is 0.39, ranging between 0.26 and 0.49.

Among the exponential regression group, most (57%) of the flux data by Exp1 were smaller than those of Exp2, with a mean ratio of F_{Exp1} /F_{Exp2} = 0.95. These underestimated values occurred mainly at MB and NS. Note that F_{Exp1} was even closer to F_{Lin2} than to F_{Exp2} in the afternoon at NS (Fig. 5d), because the fitted slopes by Exp1 had large RMSE (Fig. 4). If we reject the fitted measurement with a smaller RMSE threshold, then the curve of Exp1 in Fig. 5d would be closer to Exp2 and Exp3, which is not shown. The best agreement with Exp2 among the

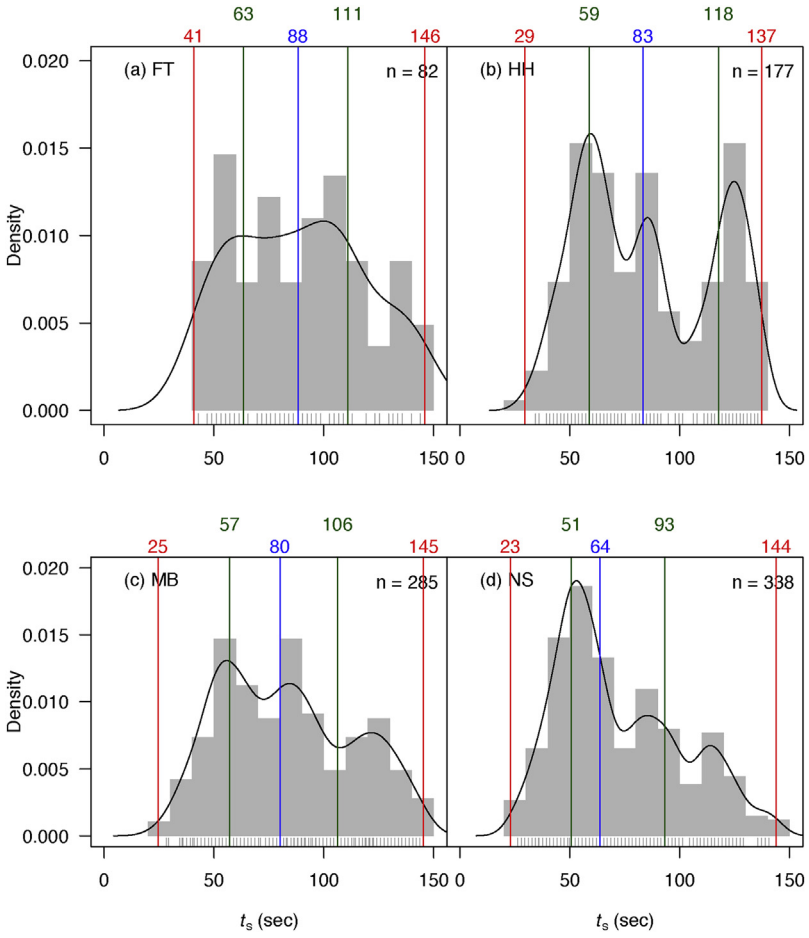

Fig. 2. Distribution of the stationary-point time (t_s) at FT (a), HH (b), MB (c), and NS (d). n is the sample size. Vertical lines indicate the median (blue), the first and third quartiles (green), and the minimum and maximum (red). (For interpretation of the references to color in this figure legend, the reader is referred to the web version of this article.)

exponential regression is for Exp3. The ratio F_{Exp3} / F_{Exp2} had a mean of 1.01 and a range between 0.87 and 1.22. The flux values by Exp3 were close to those by Exp2 at MB and NS. Large values of F_{Exp3} mostly occurred at FT site with F_{Exp3}/F_{Exp2} ranging from 0.96 to 1.22. At HH site, F_{Exp3} /F_{Exp2} ranged between 0.91 to 1.03, when most (71%) fluxes by Exp3 were smaller than those by Exp2.

In the literature, Kutzbach et al. (2007) reported that the CO_2 flux estimated by linear regression can be as low as 40% compared to that by exponential regression for observation times of only 2 min. Kroon et al. (2008) demonstrated that the linear regression method underestimated the N_2O flux by 20% at a sampling time of 3 min, and this underestimation increased drastically with time. Our study suggested that the linear regression in automated transparent chambers must be abandoned, as it gives poor goodness-of-fit statistics and underestimates the CO_2 flux by as much as 60–70% compared to the exponential regression even for short observation times of 1-2 minutes.

4. Conclusion

The problems of the automated transparent chamber technique for CO_2 flux measurement were addressed in this study. Field campaigns were carried out at four alpine grasslands, with linear regression and exponential regression methods as well as different observation time choices applied for flux estimation.

The goodness-of-fit statistics showed that the linear method dramatically biased the chamber CO_2 mixing ratio evolution, which was around 32–39% of the flux by the exponential method. The nonlinear change in CO_2 mixing ratio in the transparent chambers started shortly after the chamber was closed. Shortening the observation time to 1-2 min did not improve the regression. Therefore, it is suggested that the linear regression method should be abandoned in transparent chamber measurement for daytime CO_2 fluxes.

Abnormal behavior of CO_2 concentration time series in the chambers could be explained by the so-called Clouded Glass Effect (CGE), i.e. condensed water drops on the inner wall of the chamber dome, due to the evapotranspiration of the soil and vegetation. Affected by the CGE, the determination of the observation time is critical to the performance of the exponential regression methods. A 150-s observation time (Exp1) underestimated the chamber CO_2 flux by 5% compared to the flux estimated from a short observation time which is determined by the mathematic stationary point in CO_2 mixing ratio time series (Exp2).

In order to avoid the influence of the CGE on flux estimation, care must be taken with automated transparent chambers for trace-gas flux measurement, especially in humid areas or regions with high evapotranspiration. Therefore we propose the following suggestions.

(1) Automated clear chamber systems should be configured to measure long enough ($\leq$ 150 s according to this study), so that the users can have the chance to apply any of the proposed (or future) methods to account for the CGE or other effects. The drawback is that the online computed outcomes (in case of LI-8100A) will not be reliable when the time series include the mixing ratio measurements longer than t_s. Then post-processing will be the default configuration.
(2) The observation time might be chosen visually, but a long-term measurements could collect a large dataset, then the fourth-order polynomial can be an automated method to find the stationary-point time in the CO_2 mixing ratio time series (Exp2), which was demonstrated to improve the exponential regression remarkably.
(3) The linear term in Eq. (7) accounting for the reversal in CO_2 concentration (Exp3) can better fit the CO_2 mixing ratio evolution. As

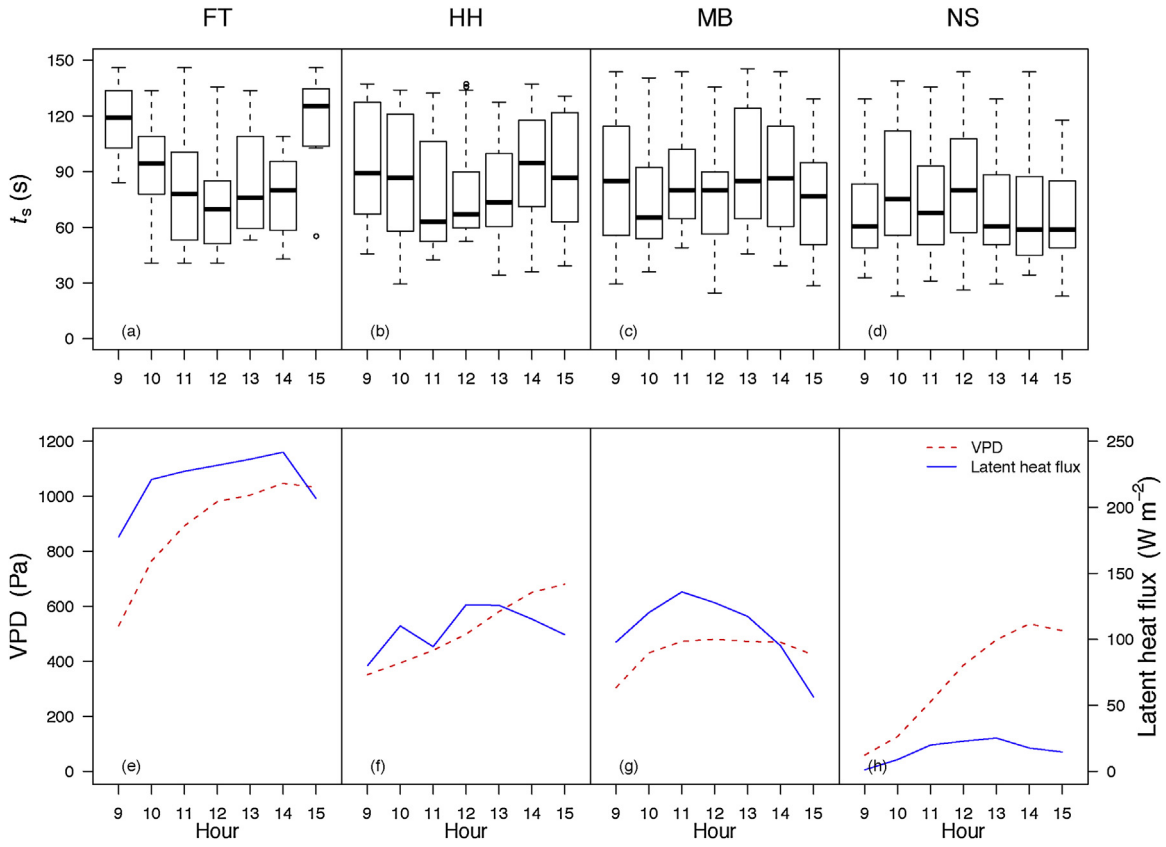

Fig. 3. Diurnal patterns of the stationary-point time (t_s) (boxplots), latent heat fluxes (blue lines), and ambient vapor pressure deficit (VPD, red dash lines). The boxplots are composed of the median (solid line), the lower quartile and upper quartile (box), the lowest datum still within 1.5 times of interquartile range (IQR) of the lower quartile, and the highest datum still within 1.5 IQR of the upper quartile (markers). (For interpretation of the references to color in this figure legend, the reader is referred to the web version of this article.)

the goodness-of-fit statistics showed that the exponential regression in Eq. (7) performed close to Exp2, Exp3 could represent an alternative to estimate the CO_2 flux and the influence of CGE on flux calculation.

(4) The condensation on chamber domes can easily be detected with manual chambers, but such information is currently missing for automated chambers, which are designed for long term unattended measurements. New techniques in hardware are expected to solve

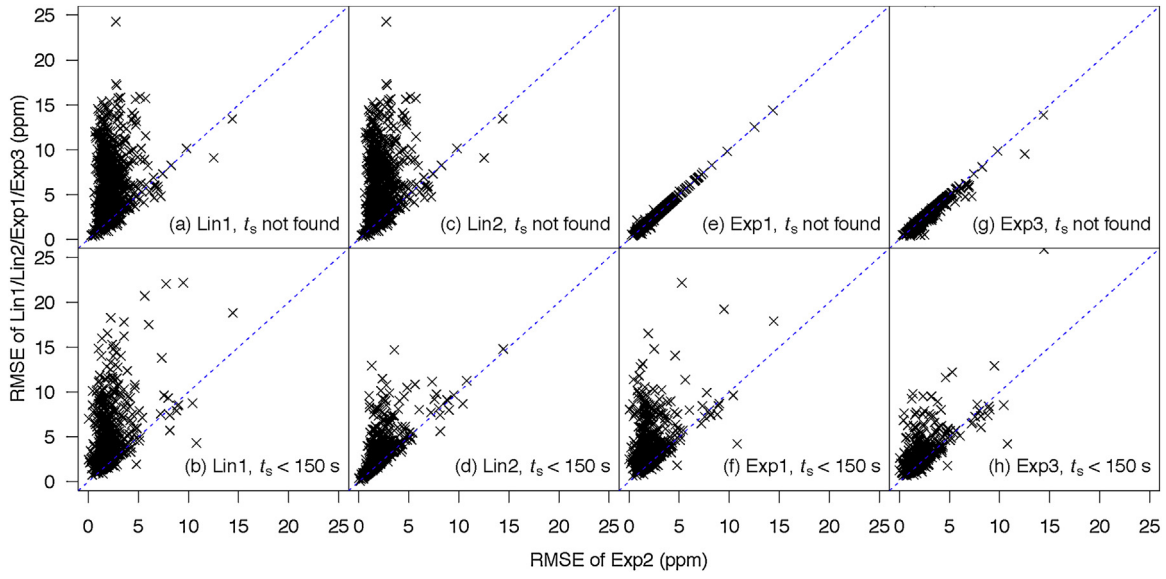

Fig. 4. Comparisons of the Lin1 regression (a, b), the Lin2 regression (c, d), the Exp1 regression (e, f) and the Exp3 regression (g, h) against the Exp2 regression by the root mean square error (RMSE). The upper panel indicates the data with the stationary point time t_s not found in the 150-s measurement, and the lower indicates the data with t_s < 150 s found. The blue dotted line is the 1:1 line. (For interpretation of the references to color in this figure legend, the reader is referred to the web version of this article.)

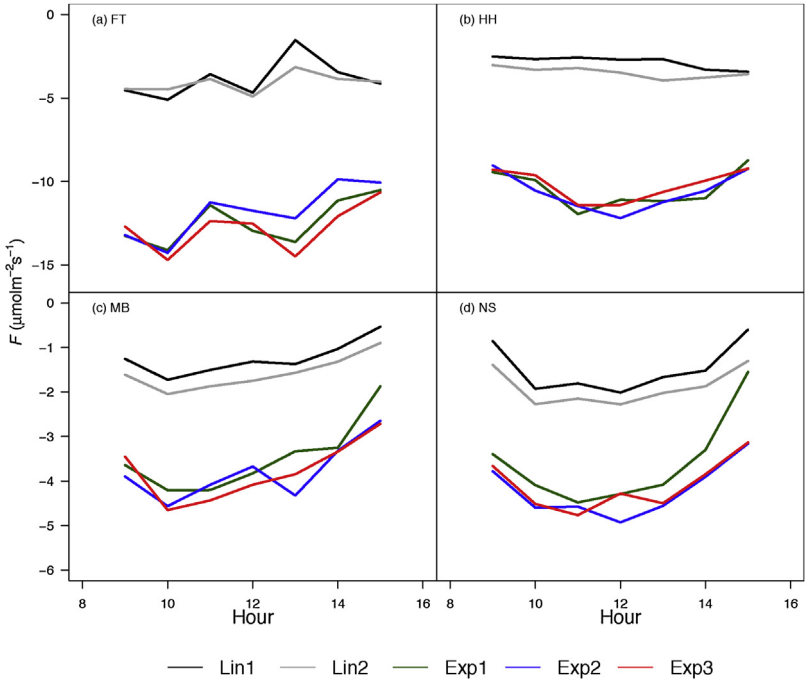

Fig. 5. Comparison of daytime CO_2 fluxes of all regression (black: Lin1; gray: Lin2; green: Exp1; blue: Exp2; red: Exp3) algorithms for four sites. (For interpretation of the references to color in this figure legend, the reader is referred to the web version of this article.)

the CGE, such as additional solar radiation measurements under the chamber dome as a quality control information, or auxiliary desiccants which can avoid the condensation on the inner wall of the chamber dome.

Acknowledgement

We are grateful to the colleagues from the Biomet group, Institute of Ecology, University of Innsbruck for support during the field work. We appreciate the support from Edmund Mach Foundation. This study was funded by the Austrian Science Fund (FWF, P26425-B16). The TERrestrial Environmental Observatory (TERENO) pre-Alpine infrastructure is funded by the Helmholtz Association and the Federal Ministry of Education and Research. We thank the Scientific Team of ScaleX Campaign 2016 for their contribution. Matthias Zeeman received support from the German Research Foundation (DFG; project ZE1006/2-1).

References

Brændholt, A., Steenberg Larsen, K., Ibrom, A., Pilegaard, K., 2017. Overestimation of closed-chamber soil CO_2 effluxes at low atmospheric turbulence. Biogeosciences 14, 1603–1616. https://doi.org/10.5194/bg-14-1603-2017. https://www.biogeosciences.net/14/1603/2017/.

De Mello, W.Z., Hines, M.E., 1994. Application of static and dynamic enclosures for determining dimethyl sulfide and carbonyl sulfide exchange in sphagnum peatlands: implications for the magnitude and direction of flux. J. Geophys. Res.: Atmos. 99, 14601–14607. https://doi.org/10.1029/94JD01025.

Denmead, O.T., 2008. Approaches to measuring fluxes of methane and nitrous oxide between landscapes and the atmosphere. Plant Soil 309, 5–24. https://doi.org/10.1007/s11104-008-9599-z.

Farquhar, G.D., von Caemmerer, S., Berry, J.A., 1980. A biochemical model of photosynthetic CO_2 assimilation in leaves of C3 species. Planta 149, 78–90. https://doi.org/10.1007/BF00386231.

Galvagno, M., Wohlfahrt, G., Cremonese, E., Filippa, G., Migliavacca, M., di Cella, U.M., van Gorsel, E., 2017. Contribution of advection to nighttime ecosystem respiration at a mountain grassland in complex terrain. Agric. For. Meteorol. 237–238, 270–281. https://doi.org/10.1016/j.agrformet.2017.02.018. http://www.sciencedirect.com/science/article/pii/S0168192317300515.

Görres, C.-M., Kammann, C., Ceulemans, R., 2016. Automation of soil flux chamber measurements: potentials and pitfalls. Biogeosciences 13, 1949–1966. https://doi.org/10.5194/bg-13-1949-2016. https://www.biogeosciences.net/13/1949/2016/.

Guidolotti, G., De Dato, G., Liberati, D., De Angelis, P., 2017. Canopy chamber: a useful tool to monitor the CO_2 exchange dynamics of shrubland. iForest - Biogeosc. For. 597–604. https://doi.org/10.3832/ifor2209-010. http://www.sisef.it/iforest/contents/?id=ifor2209-010.

Hammerle, A., Haslwanter, A., Schmitt, M., Bahn, M., Tappeiner, U., Cernusca, A., Wohlfahrt, G., 2007. Eddy covariance measurements of carbon dioxide, latent and sensible energy fluxes above a meadow on a mountain slope. Bound. Layer Meteorol. 122, 397–416.

Hendriks, D., Van Huissteden, J., Dolman, A., 2010. Multi-technique assessment of spatial and temporal variability of methane fluxes in a peat meadow. Agric. For. Meteorol. 150, 757–774.

Hendriks, D.M.D., van Huissteden, J., Dolman, A.J., van der Molen, M.K., 2007. The full greenhouse gas balance of an abandoned peat meadow. Biogeosciences 4, 411–424. https://doi.org/10.5194/bg-4-411-2007. https://www.biogeosciences.net/4/411/2007/.

Koskinen, M., Minkkinen, K., Ojanen, P., Kämäräinen, M., Laurila, T., Lohila, A., 2014. Measurements of CO_2 exchange with an automated chamber system throughout the year: challenges in measuring night-time respiration on porous peat soil. Biogeosciences 11, 347–363. https://doi.org/10.5194/bg-11-347-2014. https://www.biogeosciences.net/11/347/2014/.

Kostyanovsky, K., Huggins, D., Stockle, C., Waldo, S., Lamb, B., 2018. Developing a flow through chamber system for automated measurements of soil N_2O and CO_2 emissions. Measurement 113, 172–180. https://doi.org/10.1016/j.measurement.2017.05.040. http://www.sciencedirect.com/science/article/pii/S0263224117303287.

Kroon, P.S., Hensen, A., van den Bulk, W.C.M., Jongejan, P.A.C., Vermeulen, A.T., 2008. The importance of reducing the systematic error due to non-linearity in N_2O flux measurements by static chambers. Nutr. Cycl. Agroecosyst. 82, 175–186. https://doi.org/10.1007/s10705-008-9179-x.

Kutzbach, L., Schneider, J., Sachs, T., Giebels, M., Nykänen, H., Shurpali, N., Martikainen, P., Alm, J., Wilmking, M., 2007. CO_2 flux determination by closed-chamber methods can be seriously biased by inappropriate application of linear regression. Biogeosciences 4, 1005–1025.

LI-COR, 2010. Li-8100a Automated Soil CO_2 Flux System & Li-8150 Multiplexer Instruction Manual.

Livingston, G.P., Hutchinson, G.L., Spartalian, K., 2006. Trace gas emission in chambers. Soil Sci. Soc. Am. J. 70, 1459–1469.

Lüers, J., Detsch, F., Zhao, P., 2014. Application of a Multi-Step Error Filter for Post-Processing Atmospheric Flux and Meteorological Basic Data. University of Bayreuth, Department of Micrometeorology ISSN 1614-8916. Work Report 58, 22 pp.

Marcolla, B., Cescatti, A., Manca, G., Zorer, R., Cavagna, M., Fiora, A., Gianelle, D., Rodeghiero, M., Sottocornola, M., Zampedri, R., 2011. Climatic controls and ecosystem responses drive the inter-annual variability of the net ecosystem exchange of an alpine meadow. Agric. For. Meteorol. 151, 1233–1243. https://doi.org/10.1016/j.agrformet.2011.04.015. http://www.sciencedirect.com/science/article/pii/S0168192311001444.

Matthias, A.D., Yarger, D.N., Weinbeck, R.S., 1978. A numerical evaluation of chamber methods for determining gas fluxes. Geophys. Res. Lett. 5, 765–768. https://doi.org/10.1029/GL005i009p00765.

Mauder, M., Cuntz, M., Drüe, C., Graf, A., Rebmann, C., Schmid, H., Schmidt, M., Steinbrecher, R., 2013. A strategy for quality and uncertainty assessment of long-term

eddy-covariance measurements. Agric. For. Meteorol. 169, 122–135.
Moffat, A.M., Brümmer, C., 2017. Improved parameterization of the commonly used exponential equation for calculating soil–atmosphere exchange fluxes from closed-chamber measurements. Agric. For. Meteorol. 240–241, 18–25. https://doi.org/10.1016/j.agrformet.2017.03.00. http://www.sciencedirect.com/science/article/pii/S0168192317300850.
Pihlatie, M.K., Christiansen, J.R., Aaltonen, H., Korhonen, J.F., Nordbo, A., Rasilo, T., Benanti, G., Giebels, M., Helmy, M., Sheehy, J., Jones, S., Juszczak, R., Klefoth, R., do Vale, R.L., Rosa, A.P., Schreiber, P., Serça, D., Vicca, S., Wolf, B., Pumpanen, J., 2013. Comparison of static chambers to measure CH_4 emissions from soils. Agric. For. Meteorol. 71–172, 124–136. https://doi.org/10.1016/j.agrformet.2012.11.008. http://www.sciencedirect.com/science/article/pii/S0168192312003450.
R Core Team, 2016. R: A Language and Environment for Statistical Computing. R Foundation for Statistical Computing, Vienna, Austria. https://www.R-project.org/.
Riederer, M., Serafimovich, A., Foken, T., 2014. Net ecosystem CO_2 exchange measurements by the closed chamber method and the eddy covariance technique and their dependence on atmospheric conditions. Atmos. Meas. Tech. 7, 1057–1064. https://doi.org/10.5194/amt-7-1057-2014. http://www.atmos-meas-tech.net/7/1057/2014/.
Rochette, P., Hutchinson, G.L., 2005. Measurement of soil respiration in situ: chamber techniques. Micrometeorol. Agric. Syst. 247–286.
Rotach, M.W., Stiperski, I., Fuhrer, O., Goger, B., Gohm, A., Obleitner, F., Rau, G., Sfyri, E., Vergeiner, J., 2017. Investigating exchange processes over complex topography: the Innsbruck Box (i-Box). Bull. Am. Meteor. Soc. 98, 787–805.
Savage, K., Davidson, E.A., Richardson, A.D., 2008. A conceptual and practical approach to data quality and analysis procedures for high-frequency soil respiration measurements. Funct. Ecol. 22, 1000–1007. https://doi.org/10.1111/j.1365-2435.2008.01414.x.
Savage, K., Phillips, R., Davidson, E., 2014. High temporal frequency measurements of greenhouse gas emissions from soils. Biogeosciences 11, 2709–2720. https://doi.org/10.5194/bg-11-2709-2014. https://www.biogeosciences.net/11/2709/2014/.
Vargas, R., Carbone, M.S., Reichstein, M., Baldocchi, D.D., 2011. Frontiers and challenges in soil respiration research: from measurements to model-data integration. Biogeochemistry 102, 1–13. https://doi.org/10.1007/s10533-010-9462-1.
Wohlfahrt, G., Anfang, C., Bahn, M., Haslwanter, A., Newesely, C., Schmitt, M., Drösler, M., Pfadenhauer, J., Cernusca, A., 2005. Quantifying nighttime ecosystem respiration of a meadow using eddy covariance, chambers and modelling. Agric. For. Meteorol. 128, 141–162. https://doi.org/10.1016/j.agrformet.2004.11.003. http://www.sciencedirect.com/science/article/pii/S0168192304003028.
Wohlfahrt, G., Hammerle, A., Haslwanter, A., Bahn, M., Tappeiner, U., Cernusca, A., 2008. Seasonal and inter-annual variability of the net ecosystem CO_2 exchange of a temperate mountain grassland: effects of weather and management. J. Geophys. Res. 113. https://doi.org/10.1029/2007JD009286.
Wolf, B., Chwala, C., Fersch, B., Garvelmann, J., Junkermann, W., Zeeman, M.J., Angerer, A., Adler, B., Beck, C., Brosy, C., Brugger, P., Emeis, S., Dannenmann, M., Roo, F.D., Diaz-Pines, E., Haas, E., Hagen, M., Hajnsek, I., Jacobeit, J., Jagdhuber, T., Kalthoff, N., Kiese, R., Kunstmann, H., Kosak, O., Krieg, R., Malchow, C., Mauder, M., Merz, R., Notarnicola, C., Philipp, A., Reif, W., Reineke, S., Rödiger, T., Ruehr, N., Schäfer, K., Schrön, M., Senatore, A., Shupe, H., Völksch, I., Wanninger, C., Zacharias, S., Schmid, H.P., 2017. The SCALEX campaign: scale-crossing land surface and boundary layer processes in the TERENO-preAlpine Observatory. Bull. Am. Meteorol. Soc. 98, 1217–1234. https://doi.org/10.1175/BAMS-D-15-00277.1.
Xu, L., Furtaw, M.D., Madsen, R.A., Garcia, R.L., Anderson, D.J., McDermitt, D.K., 2006. On maintaining pressure equilibrium between a soil CO_2 flux chamber and the ambient air. J. Geophys. Res.: Atmos. 111. https://doi.org/10.1029/2005JD006435.
Zacharias, S., Bogena, H., Samaniego, L., Mauder, M., Fuß, R., Pütz, T., Frenzel, M., Schwank, M., Baessler, C., Butterbach-Bahl, K., Bens, O., Borg, E., Brauer, A., Dietrich, P., Hajnsek, I., Helle, G., Kiese, R., Kunstmann, H., Klotz, S., Vereecken, H., 2011. A Network of Terrestrial Environmental Observatories in Germany, vol. 10. pp. 955–973.
Zeeman, M., Mauder, M., Steinbrecher, R., Heidbach, K., Eckart, E., Schmid, H., 2017. Reduced snow cover affects productivity of upland temperate grasslands. Agric. For. Meteorol. 232, 514–526. https://doi.org/10.1016/j.agrformet.2016.09.002. http://www.sciencedirect.com/science/article/pii/S0168192316303811.
Zhao, P., Lüers, J., 2016. Improved data gap-filling schemes for estimation of net ecosystem exchange in typical east-asian croplands. Sci. China Earth Sci. 1–13. https://doi.org/10.1007/s11430-015-0192-1.